

Design Status of the ITER Upper Port Launcher

M.A. Henderson¹, R. Chavan¹, R. Bertizzolo¹, A. Bruschi², E. Ciattaglia³, S. Cirant²,
A. Collazos¹, I. Danilov⁴, F. Dolizy¹, J. Duron¹, D. Farina², R. Heidinger⁴, J.-D.
Landis¹, A. Moro², P. Platania², E. Poli⁵, G. Ramponi², G. Saibene³, F. Sanchez¹,
O. Sauter¹, A. Serikov⁴, H. Shidara¹, P. Spaeh⁴, V.S. Udintsev¹, H. Zohm⁵

¹ CRPP, EURATOM – Confédération Suisse, EPFL, CH-1015 Lausanne Switzerland

² Istituto di Fisica del Plasma, EURATOM- ENEA- CNR, 20125 Milano, Italy

³ EFDA Close Support Unit, Boltzmannstrasse 2, D-85748 Garching, Germany

⁴ Forschungszentrum Karlsruhe, EURATOM-FZK, D-76021 Karlsruhe, Germany

⁵ Max Planck-Institute für Plasmaphysik, EURATOM-IPP, D-85748 Garching,
Germany

First Author e-mail: mark.henderson@epfl.ch

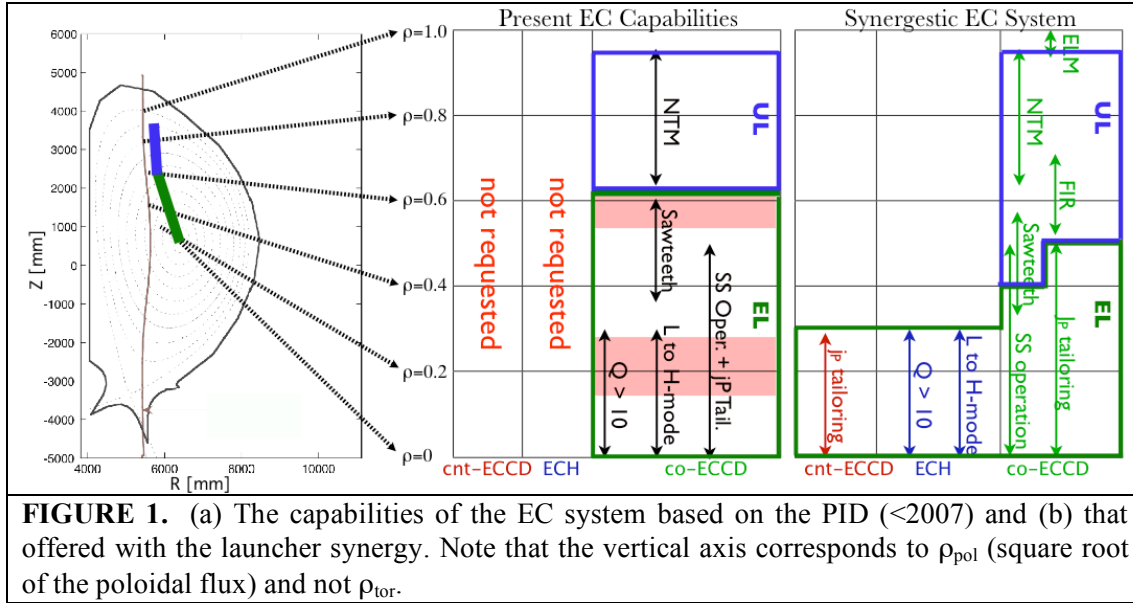
Abstract

The purpose of the ITER ECRH upper port antenna (or launcher) will be to drive current locally to stabilise the NTMs (depositing ECCD inside of the island that forms on either the $q=3/2$ or 2 rational magnetic flux surfaces) and control the sawtooth instability (deposit ECCD near the $q=1$ surface). The launcher should be capable of steering the focused beam deposition location to the resonant flux surface over the range in which the $q=1$, $3/2$ and 2 surfaces are expected to be found, for the various plasma equilibria susceptible to the onset of NTMs and sawteeth. ITER's present reference design uses a front steering (FS) concept, with the moveable mirror close to the plasma. Two separate mirrors are used to decouple the focussing and steering aspects resulting in an optimised optical configuration providing a well focused beam over a large steering range. The launcher is capable of steering eight 2MW beams in all of the four allocated upper port plugs. Details of the FS launcher design relating to physics performance, mm-wave optical design and steering mechanism design are discussed in this paper.

Introduction

ITER is planned to have 24MW of installed EC power, which will be launched into the plasma via either the equatorial (EL) or upper (UL) launchers [1,2]. A remote controllable switch deviates the power to either launcher depending on the physics requirements as defined in the ITER Project Integration Document [3]. Initially, the four ports of the UL were dedicated to the single application of stabilising the neoclassical tearing modes [4] that could occur on either the $q=3/2$ or 2 flux surfaces in the relevant scenarios 2, 3a and 5. This translates into a steering range accessing $0.52 \leq \rho_{\text{tor}} \leq 0.85$, where ρ_{tor} being the square root of the normalized toroidal flux. This steering range provided an adequate coverage to accommodate the uncertainties of the flux surfaces that will one day be realised in ITER. The single port of the EL was dedicated to all other physics applications (sawtooth control, central heating and current drive) as illustrated in figure 1a.

This partitioning of applications had several shortcomings, mainly because the single port EL was given the majority of the physics applications, while the four port UL was dedicated to the single task of NTM stabilisation. The EL required a relatively large steering range accessing from on axis to $\rho_{\text{tor}} \sim 0.55$. Due to geometrical limitations the EL could not deposit the full power over the entire steering range and resulted in less than 100% full pass absorption in the outer 20% of its steering range [5] (see red band regions of figure 1a)



A revision of the physics objectives was proposed in Ref. [6] that partitioned the applications of each launcher based on the need for either a narrow current deposition (control of sawtooth [7] and NTMs) as provided by the UL or bulk current drive and central heating as provided by the EL. To achieve this, the UL had to have an increased steering range to access the $q=1$ surfaces, or into $\rho_{tor} \sim 0.3$. This alleviates the EL of the required large steering range required (to access the $q=1$) and permits the launcher to be modified for better central coverage and the potential for counter ECCD and pure heating capabilities as outlined in Ref. [6] and illustrated in figure 1b. Note that the counter ECCD is useful for control of the q -profile in advanced (scenario 3a) and reverse shear (scenario 4) scenarios [8] as well as combining with co-ECCD to provide pure heating with no net current drive as has been demonstrated on ASDEX-Upgrade [9]. Note that the EC system is the only heating and current drive source on ITER that can provide either co-ECCD, counter-ECCD or pure heating, simultaneously with the capability to vary the deposition location and all via external actuators. These functions provide minor modifications to the EL, while increasing the flexibility of the EC systems to be applicable to a greater number of plasma scenarios.

The key issue in achieving the full capabilities of the EC system (as illustrated in figure 1b) is to increase the steering range of the UL, which has been achieved in the enhanced performance launcher (EPL) design [2]. The two steering mirrors of the UL are directed to two overlapping regions in the plasma cross section, $0.3 \leq \rho_{tor} \leq 0.8$ for the upper steering mirror (USM) and $0.55 \leq \rho_{tor} \leq 0.85$ for the lower steering mirror (LSM) as illustrated in figure 2. The overall steering range of each mechanism is actually decreased to reduce the induced stresses and prolong the steering mechanism longevity prior to the onset of cyclic fatigue. Note this design was prompted by ITER-IT request that the front steering launcher design use four upper ports (even though only three ports are required for steering the 24 beams) with the fourth port used to increase the launchers functionality and reduce the engineering constraints, both of which have been achieved at the cost of an additional fourth port to the European parties procurement package. The enhanced performance offered by the revision of the UL has now been incorporated in the revised PID [10].

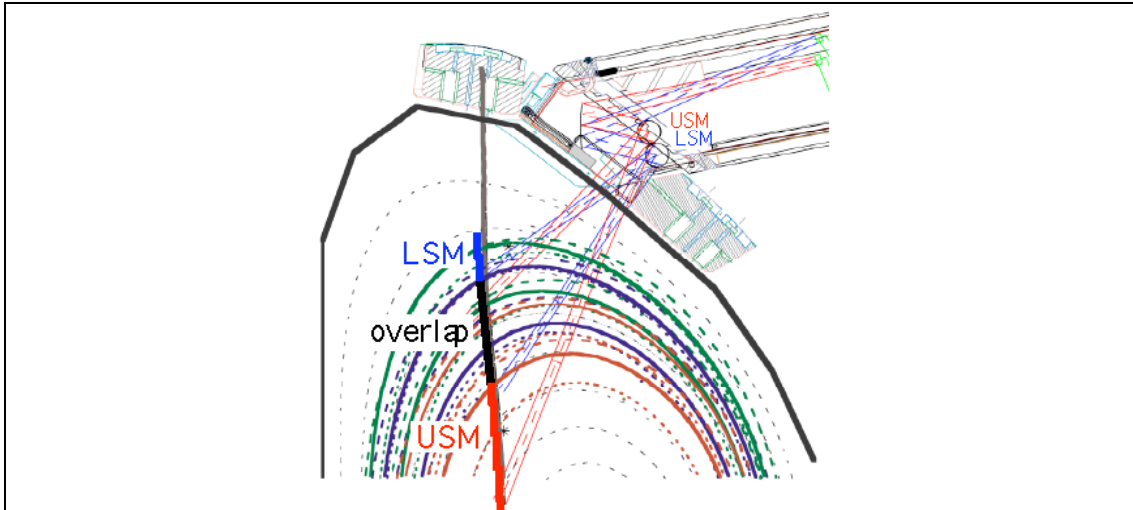


FIGURE 2. The EPL has the range of the two steering mirrors (USM and LSM) scanning two different regions such that a larger region in the plasma is accessible. Each steering mirror can inject up to 13.3MW, the full 20MW can be deposited in the overlap region.

Enhanced Performance UL design

A simplified view of the current FS launcher design is shown in Figure 3. Eight circular HE_{11} waveguides ($\phi_{WG}=63.5\text{mm}$, similar to the waveguide used in the transmission line) enter the port plug entrance on the right (note that there are four waveguides superimposed in this poloidal cut). Prior to the closure plate a diamond window and an in-line isolation valve is placed to provide the primary tritium barrier. The waveguide continue after the closure plate to a set of miter bends in a ‘dog-leg’ configuration used to angle the 8 beams (both in toroidal and poloidal directions) to two focusing mirrors with the incident beams partially overlapping in both toroidal and poloidal directions. The reflected beams are then directed downward to two flat steering mirrors, which redirect the beams into the plasma with a toroidal injection angle of $\beta \approx 20^\circ$.

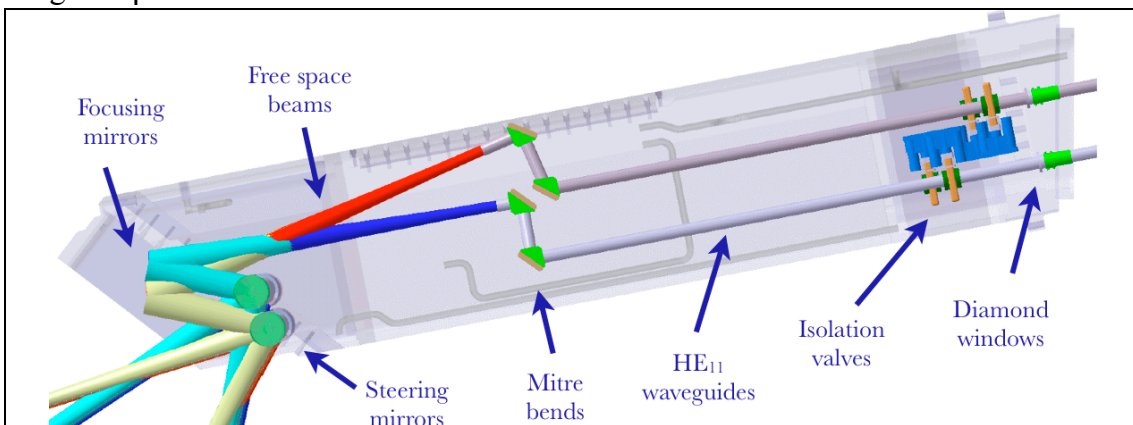


FIGURE 3. The layout of the principle mm-wave components of the upper launcher.

The deposition region of the two UL steering mirrors are displaced so that the upper steering mirror (USM) access further inward providing access to the inner NTMs and $q=1$ surfaces covering a range of $\sim 0.3 \leq \rho_{\text{tor}} \leq \sim 0.8$, while the lower steering mirror (LSM) access the outer NTMs covering a range of $\sim 0.55 \leq \rho_{\text{tor}} \leq 0.85$. An additional switching system is used prior to the port entrance that can deviate the beams coming from the 24 gyrotrons to either the 16 entrances associated with the USM or the 16 entrances with the LSM depending on the physics requirements. The

optical design is optimized [11] so that the beam from the USM projects a slightly larger beam waist (29mm) further into the plasma to compensate for the longer path length as compared to the LSM with a waist of 21mm. This process was performed with dedicated beam tracing scans system [5,12] to insure a narrow and peaked j_{CD} profile over the entire steering range. Note that four beams are incident on a single focusing and steering mirror, the overlapping of the beams permit the largest beam for a finite focusing mirror size within the confined space of the blanket shield module (BSM). The space in the BSM is shared between the mm-wave components and shield blocks to protect the components and port plug from the neutron flux. Nuclear analysis of the EPL has demonstrated that there is adequate shielding to protect both the critical components of the launcher and neighboring components [13].

Alternative configurations are under investigation to either improve the physics performance of the launcher, reduce complexity and/or to enhance maintenance access. For example, relocating the valves and windows located several meters from the closure plate alleviates the congestion at the port plug entrance and enhances the maintenance access to these components. Also replacing the mitre bends with free space mirrors improves the focusing of the beams for improved NTM stabilization efficiencies, while reducing the overall cost and complexity of the optical systems. These design modifications are under consideration for the next optical design of the launcher, which is expected for the end of 2007.

Steering Mechanism design

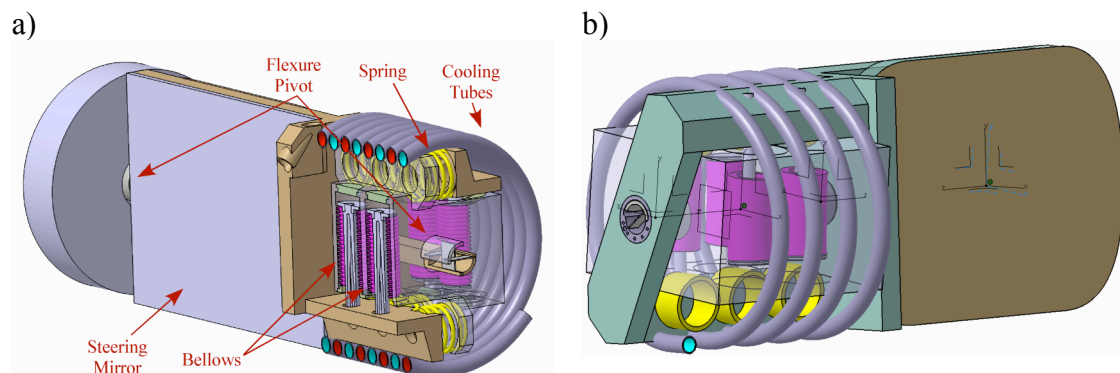


FIGURE 4 a) The ‘balanced’ and b) ‘cantilevered’ steering mechanism designs.

The steering mirror ensemble is the most critical component of the upper launcher and is the most likely component to encounter mechanical problems. In order to minimize these risks, an innovative design of the steering mechanism [14,15] (see Figure 2a) is being developed that provides rotation of the steering mirror based on the compliant deformation of structural components offering a frictionless and backlash free mechanical movement and avoiding the in vessel tribological difficulties inherent in present day steering mechanisms. Traditional ball bearings are replaced with elastically compliant flexure pivots and the movement is controlled using an integrated gaseous helium pneumatic actuator system working against preloaded compressive springs in place of the push-pull rods. This eliminates the components that typically grip offering an improved reliability and precision in controlling the steering mirror angle. The bellows are pressurized from the outside, which offers a more stable configuration avoiding the squirm instability when the bellows are internally pressurized. A pair of coiled cooling pipes with either a single or double wall provides a flexible coolant feed to the mirror, following a similar design to that proposed for the EL [1].

The steering mirror (SM) ensemble of figure 4a is referred to as the ‘balanced SM’, which has the SM centered between two flexure pivots. This configuration reduces the overall forces on the flexure pivots during a vertical disruption event (VDE), but increases the risk of halo current flowing through the mirror structure and requires two supports on either side of the SM. An alternative configuration is the ‘cantilevered’ SM as shown in figure 4b, with both flexure pivots incorporated in the steering mechanism. This configuration was the original SM design back in 2003, but compatible for only two 1MW incident beams. The balanced SM was chosen because it is compatible with four 2MW and could compensate for the additional forces associated with the larger mirror. Optimizing the mirror design for lower induced currents during a VDE reduces the forces on the flexure pivots, which then allow the cantilevered SM to be reconsidered, simplifying the installation and repair of the SM. Both designs are being progressed to the manufacturing design level, with a choice between the two configurations is planned before 2008.

Acknowledgments

This work, supported by the Swiss National Science Foundation and the European Communities, was carried out within the framework of the European Fusion Development Agreement (ECHULA subtask (f) /contract EFDA TCP 341-22 and ECHULB subtask (b) /contract EFDA 05-1228). The views and opinions expressed herein do not necessarily reflect those of the European Commission.

References

1. K. Takahashi *et al*, Fusion Science and Technology **47** (2005) p1.
2. M.A. Henderson *et al*, *Critical Design Issues of the ITER ECH FS Upper Launcher*, to be published in Fusion Science and Technology January, 2008.
3. J. How, P. Barabaschi, W. Spears Project Integration Document, G A0 GDRD 6 04-09-09 R0.2.
4. S. Günter *et al*, Phys. Rev. Lett. **87** (2001) 275001-1.
5. G. Ramponi *et al*, *ITER ECRH/ECCD System Capabilities for Extended Physics Applications*, to appear on Fusion Science and Technology, August 2007
6. M. Henderson *et al*, Proc. of the 14th Joint Workshop on ECE and ECRH, Santorini, Greece (2006).
7. J. Graves *et al*, Plasma Phys. Control. Fusion **47** (2005) B121-B133.
8. G. Ramponi *et al*, “Physics Analysis to Optimize the Performance of the ITER ECW System”, this conference.
9. A. Manini *et al*, Proc. of the 14th Joint Workshop on ECE and ECRH, Santorini, Greece (2006).
10. J. How, Project Integration Document, ITER_D_2234RH Version 3.0 26-01-2007.
11. H. Shidara *et al*, Proc. of the 14th Joint Workshop on ECE and ECRH, Santorini, Greece (2006).
12. E. Poli *et al*, Proc. of the 14th Joint Workshop on ECE and ECRH, Santorini, Greece (2006).
13. A. Serikov *et al*, “Radiation shield analyses in support of the FS design for the ITER ECRH launcher”, accepted for publication in Fusion Eng. Design (2007).
14. R. Chavan *et al*, Journal of Physics: Conference Series **25** (2005) 151-158.
15. J.-D. Landis *et al*, “Design of the critical components in the ITER ECH upper launcher steering mechanism”, accepted for publication in Fusion Engineering Design (2007).